

Article

Indentation Hardness and Elastic Recovery of Some Hardwood Species

Maciej Sydor ^{1,*} , Grzegorz Pinkowski ¹ , Martin Kučerka ^{2,*} , Richard Kminiak ³ , Petar Antov ⁴ 
and Tomasz Rogoziński ⁵ 

¹ Department of Woodworking Machines and Fundamentals of Machine Design, Faculty of Forestry and Wood Technology, Poznań University of Life Sciences, 60-637 Poznań, Poland; grzegorz.pinkowski@up.poznan.pl

² Faculty of Natural Sciences, Matej Bel University, 974 09 Banská Bystrica, Slovakia

³ Department of Woodworking, Faculty of Wood Science and Technology, Technical University in Zvolen, 960 01 Zvolen, Slovakia; richard.kminiak@tuzvo.sk

⁴ Faculty of Forest Industry, University of Forestry, 1797 Sofia, Bulgaria; p.antov@ltu.bg

⁵ Department of Furniture Design, Faculty of Forestry and Wood Technology, Poznań University of Life Sciences, 60-637 Poznań, Poland; tomasz.rogozinski@up.poznan.pl

* Correspondence: maciej.sydor@up.poznan.pl (M.S.); martin.kucerka@umb.sk (M.K.)

Abstract: The purpose of the study was to measure the Brinell hardness (HB) of six wood species and evaluate the ability to recover the depth of the imprint (self-re-deformation). Straight-grain clear samples of ash, beech, alder, birch, iroko, and linden wood were prepared. Measurements were made in the three main reference timber cross-sections: radial (R), tangential (T), and axial/longitudinal (L) and with two measuring loads of 30 kG and 100 kG (294.2 N and 980.7 N). The tested wood species could be classified into hard (ash, beech), medium-hard (alder, birch, iroko), and soft (linden) wood species. The HBs of each tested wood species differed in the cross-sections, i.e., side hardness (R, T) and end hardness (L). Higher HB values were obtained at 100 kG load in all species and all three cross-sections. The lowest influence of the measurement force value on the HB value was revealed for the soft wood species (linden: 107–118%). This influence was visible for the other five medium-hard and hard wood species, ranging from 125% to 176%. The percentage of temporary imprint in total imprint depth (x/H) varied from 12 to 33% (linden 12–18%—the lowest self-re-deformation ability; beech 25–33%—the highest self-re-deformation ability). The results of this study underline that the higher the density of the wood, the higher the Brinell hardness, and, simultaneously, the greater the measurement force used, the higher the Brinell hardness measured. The ability of self-re-deformation in wood's R and T cross-sections depends on the wood density and the measuring force used. In contrast, this ability only depends on the wood density in the L cross-section. Those observations imply that the compaction of the cell structure during side compression is mainly non-destructive, while the longitudinal deformation of the cell structure (the buckling of cell walls and fracture of ends of the cells) is to a great degree destructive and irreversible. These results can be used in the construction and furniture sectors, especially when designing products and planning the woodworking of highly loaded wood floors and furniture elements.

Keywords: wood hardness; Brinell hardness; indentation depth; plastic deformation; elastic deformation; imprint recovery; indentation recovery; alder; linden; birch; ash; iroko; beech



Citation: Sydor, M.; Pinkowski, G.; Kučerka, M.; Kminiak, R.; Antov, P.; Rogoziński, T. Indentation Hardness and Elastic Recovery of Some Hardwood Species. *Appl. Sci.* **2022**, *12*, 5049. <https://doi.org/10.3390/app12105049>

Academic Editor: Giuseppe Lazzara

Received: 21 April 2022

Accepted: 15 May 2022

Published: 17 May 2022

Publisher's Note: MDPI stays neutral with regard to jurisdictional claims in published maps and institutional affiliations.



Copyright: © 2022 by the authors. Licensee MDPI, Basel, Switzerland. This article is an open access article distributed under the terms and conditions of the Creative Commons Attribution (CC BY) license (<https://creativecommons.org/licenses/by/4.0/>).

1. Introduction

Hardness is the ability of a material to resist localized deformation. Hardness test force can be applied by scratching, cutting, mechanical wear, bending, dynamic or static indentation. In static indentation hardness measurement methods, a non-deformable ball, pyramid, cone, cylinder, or needle-shaped indenters are applied [1–3]. The measured indentation projection area, total indentation area, indentation depth, or force needed to indent an indenter to the required depth is used for hardness calculation. The principal

wood macro-indentation hardness testing approaches are Brinell, Vickers, Rockwell, Meyer, Knoop, Shore, Leeb, and Janka. The most widely used test procedures for measuring the hardness of wood materials are the Brinell–Mörath, Janka, and Monnin methods [4], which means that rounded indenters are preferred, those that do not crack the wood. The Brinell method for wood materials is standardized in EN 1534: 2020 [5], which describes the method of testing the hardness of wood floors using a 10 mm ball indenter, and a force of 1 kN reached in 15 ± 3 s, maintained for 25 ± 5 s and then released. The imprint size measurement is performed after the load is removed, so this method concerns only the plastic imprint size. The scientific literature presents a proposal to modify the Brinell method in measuring the hardness of wood. This proposal postulates calculating the wood hardness based on the depth of the imprint under load, including both elastic and plastic components of the imprint [6,7].

In our previous study [8], the hardness of wood materials was measured using the Brinell method, and, in addition to the size of the permanent imprint (which is a measure of Brinell hardness), we also analyzed an elastic component of the imprints, i.e., one that spontaneously disappears after removing the measuring force. In this way, we tested a feature of the wood in addition to hardness: the ability to self-shallow the imprint after removing the measuring force (self-re-deformation). Analyzing the hardness and self-re-deformation ability, we concluded that tested materials could be divided into soft (beech, pine, iroko), medium-hard (merbau, common oak, maple, red oak), and hard materials, e.g., high-density fiberboards (HDF), plywood. The highest relative value of the plastic imprint in total deformation, ranging from 79 to 83%, was observed in the soft materials tested. Values ranged from 72 to 76% in medium-hard materials and only about 65% in hard materials. Therefore, hard materials exhibited the highest ability, among the materials tested, to reduce the depth of deformation immediately after force removal. A measuring force of 30 kG was used in these tests, and the hardness was measured in one wood cross-section (side hardness). Wood, a material with cylindrical orthotropy, has three perpendiculars one to another, reference main cross-sections. The main cross-sections are related to the wood grain direction: the longitudinal (L) cross-section (also called axial), the radial (R), that of its secondary growth, and the tangential (T), orthogonal to both [9]. The so-called “end hardness”, measured in the L cross-section, is higher than the “side hardness”, measured in the cross-sections R and T, which are close to each other [9–11]. This study aimed to measure the hardness of the six hardwood species in all three main cross-sections and evaluate their tendency to self-re-deformation, that is, the self-executing flattening of the measuring ball imprint.

2. Materials and Methods

The research was carried out on six hardwoods. The test samples, 30 mm × 30 mm × 20 mm in size, were made of: alder, linden, birch, ash, iroko, and beech. All logs used to prepare the test samples had a regular structure (not eccentric). The test samples were clear and made from logs without any structural defects of the wood. The logs were primarily cut into lumber according to three principal anatomical planes of reference in the stem: radial (R), tangential (T), and axial/longitudinal (L) cross-sections (Figure 1). Twelve samples were made for each of the wood species tested.

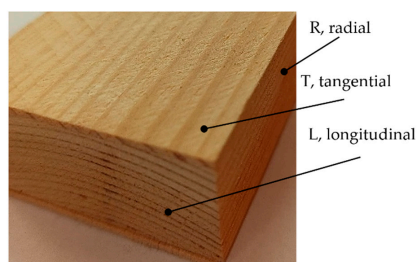


Figure 1. The clear test specimen oriented according to the main cross-sections in the stem.

After the primary cut, the planks were dried at a temperature lower than 60 °C. The test samples were cut and then conditioned at a temperature of 20 ± 2 °C and relative humidity of $65 \pm 3\%$ for three months. The moisture content of the test samples immediately before the hardness measurements was $10 \pm 0.5\%$, and their average densities are given in Table 1.

Table 1. Wood species names and average densities of test samples used.

Species	Average Density (g/cm ³)
Alder (<i>Alnus glutinosa</i> (L.) Gaertn)	0.500
Linden (<i>Tilia europaea</i> L)	0.505
Birch (<i>Betula alba</i> L.)	0.595
Ash (<i>Fraxinus excelsior</i> L.)	0.660
Iroko (<i>Milicia excelsa</i> (Welw.) CC Berg)	0.690
Beech (<i>Fagus sylvatica</i> L.)	0.740

Brinell hardness tester, model HBRV-187.5E (Huatec, Beijing, China), was used. We performed the uniaxial hardness measurements in the all three main cross-sections (R, T, and L) and used two measuring force values (30 and 100 kG). Symbolic specifications of the hardness measurement conditions HB 10/294.2/60 and HB 10/980.7/60 were assigned to both sets of test conditions, respectively:

- Measuring ball diameter $D = 10$ mm
- Total force 1 $P_{30} = 30$ kG ($F = 294.2$ N, $(F/D_{\max}^2 = 3.2)$)
- Total force 2 $P_{100} = 100$ kG ($F = 980.7$ N, $(F/D_{\max}^2 = 10.6)$)
- Partial force $P_1 = 10.0$ kG (98.07 N)
- Total load time $t = 125$ s
- Number of measurements for each material $n = 12$

Figure 2 shows the Brinell tester used and the measuring force application mode.

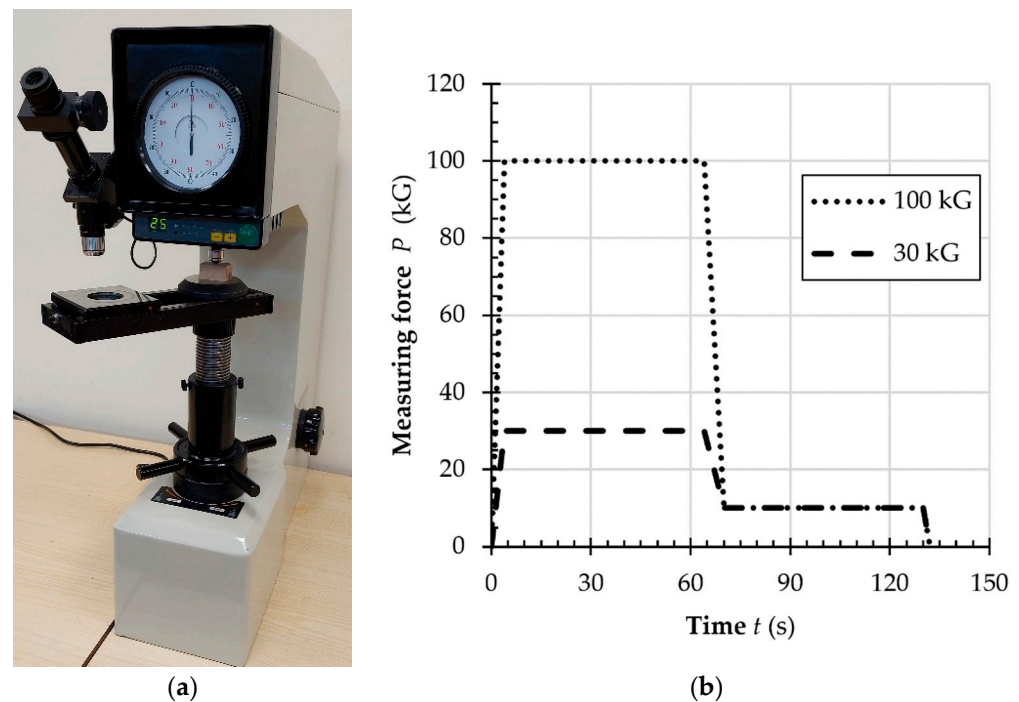


Figure 2. Hardness tester and measuring force: (a)—HBRV-187.5E Brinell hardness tester (Huatec, Beijing, China), (b)—force exertion modes.

The Brinell hardness (HB) is calculated based on the diameter of the imprint. The boundary of the imprint on the wood is unclear [8,11,12]. An additional factor that makes

hardness measurement difficult is the “sinking-in effect” [12], especially in the T and R main cross-sections of wood [7]. Therefore, we used the Dino-Lite AM4815ZT EDGE digital microscope (IDCP B.V., Almere, The Netherlands) with extended dynamic range (EDR), extended depth of field (EDOF), and the possibility of measuring under polarized light. Figure 3 shows example images taken during tests.

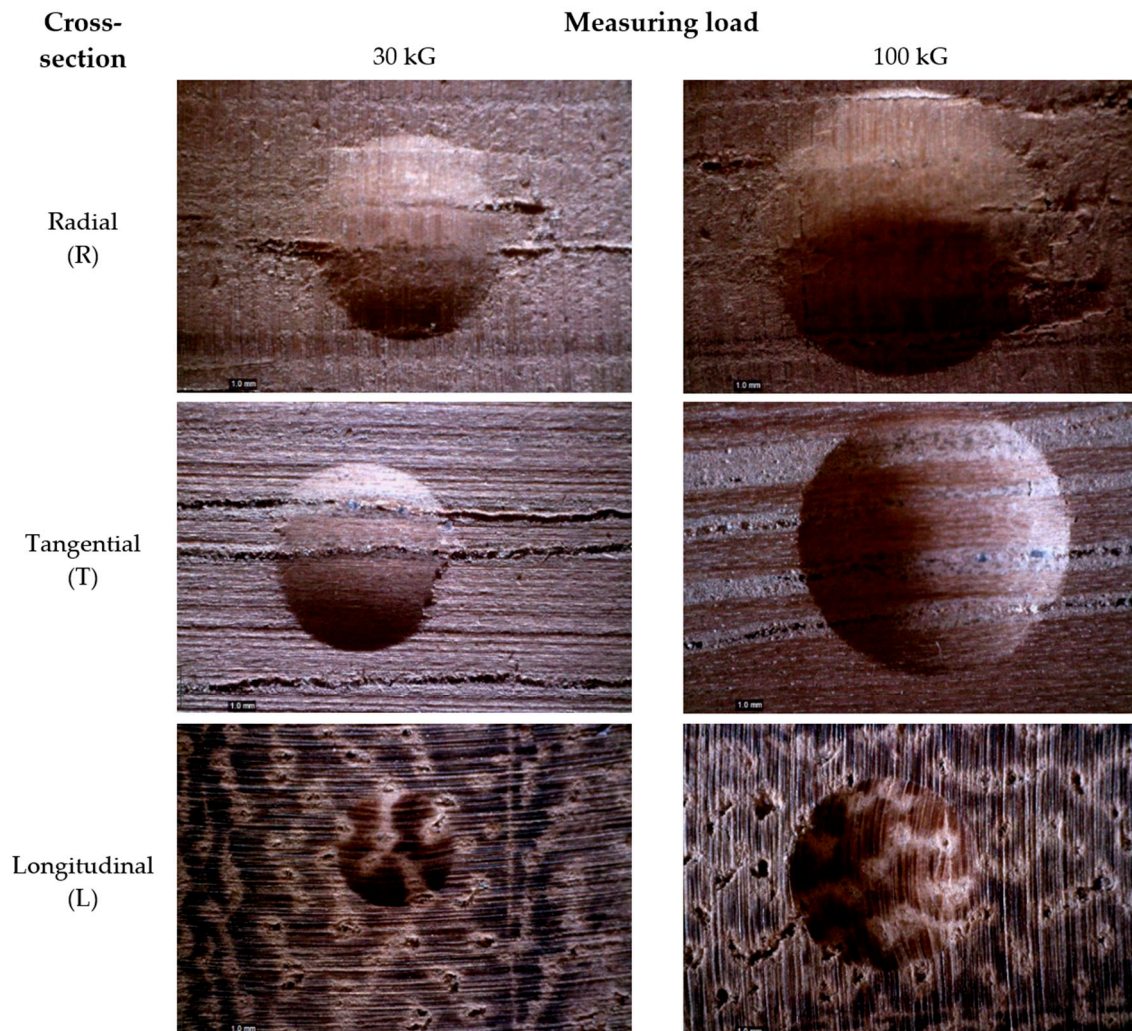


Figure 3. Examples of imprints (iroko wood, 37× magnification).

The HB values were calculated according to the following formula:

$$HB_d = \frac{2 \cdot P}{\pi \cdot D \cdot (D - \sqrt{D^2 - d^2})}$$

where:

P = applied force (kG);

D = diameter of the indenter (mm);

d = diameter of the imprint (mm).

Figure 4 shows three stages of imprint creation during the hardness test: before the loading, a ball indenter under full load, and an indenter after removing the load.

The total imprint depth (H) is the sum of the depth of the permanent imprint h (the one that remains after the measuring force P is removed) and the depth of an elastic imprint x (only under load with the measuring force P). The hardness tester used allows measuring the depth of the elastic component x of the total imprint depth, which is readable after

removing the measuring force ($x = H - h$) (Figure 4). Based on the indenter diameter (D), and the measured values of imprint diameter d , the permanent imprint depth can be calculated by the formula $h = D - \sqrt{D^2 - d^2}/2$. Based on the measured elastic component of the imprint (x), the total imprint depth can be calculated: $H = x + h$. Therefore, the force P and the diameter of the indenter D were constant; we measured d and x , and we calculated h and the hardness HB. Statistical calculations of the errors of the HB values and the imprint depth values were performed for the significance level of 95%: $\alpha = 0.05$, $n = 12$, 11 degrees of freedom, from the distribution of the t-Student: $t_{0.05,11} \approx 2.571$.

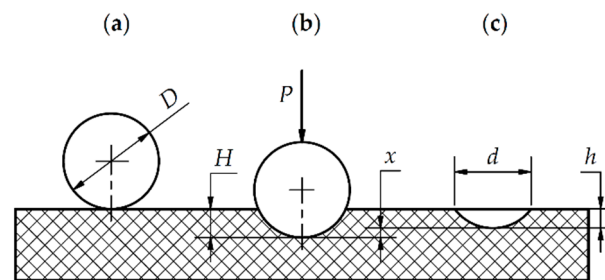


Figure 4. The imprint creation during hardness tests: (a)—stage 1, the ball without load, (b)—stage 2, the ball loaded with measuring force, (c)—stage 3, the permanent indentation after a force is removed (P —measuring force, D —diameter of the ball, d —the permanent imprint diameter, H —the total imprint depth, h —the permanent (plastic) imprint depth, x —the elastic (temporary) component of imprint depth).

3. Results

Figure 5 summarizes the calculated Brinell hardness values (HB) based on the diameter of the imprint (d). The wood species in Figure 5 are arranged according to their increased density. The HB of the test wood samples varied depending on the grain direction. The highest HB values were in the L cross-section, while the smaller values were in the R and T sections. Hardness also depends on the measuring force used. The HB measured at the force of 100 kG were greater than those measured at 30 kG.

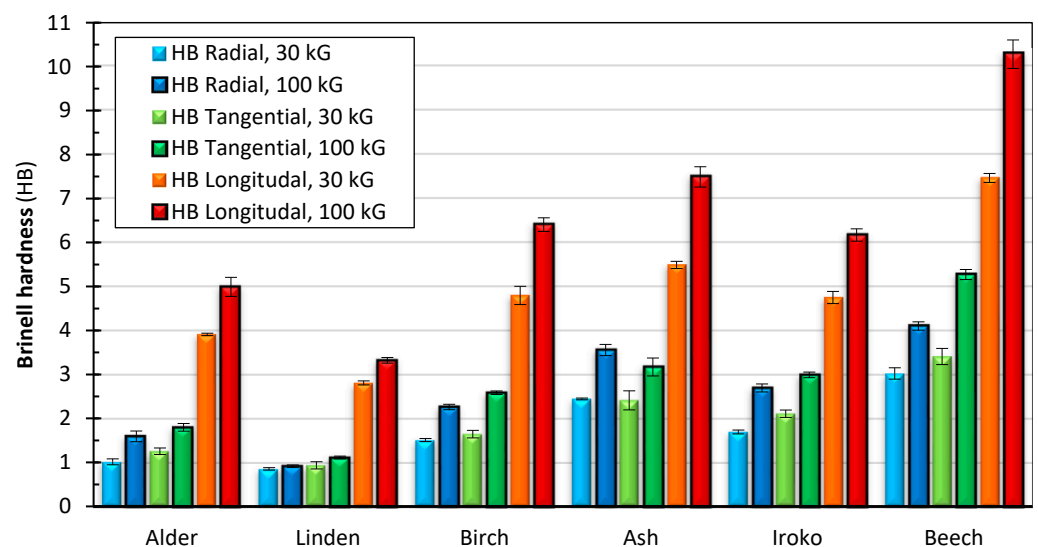


Figure 5. The Brinell hardness of the tested wood in the three main cross-sections of wood at two measuring forces (30 kG and 100 kG).

The computed hardness confidence intervals (shown as error bars in Figure 5) had varying widths. With a measuring force of 30 kG in the R cross-section, they ranged from 2% to 13% (average 7%) of hardness, in the T cross-section from 8% to 18% (average 13%), and in the L section from 1% to 9 (average 4%). However, with a measuring force of 100 kG,

the confidence intervals ranged: in the R cross-section from 3% to 13% (average 12%), in the T cross-section from 5% to 15% (average 8%) and in the L cross-section from 4% to 9% (6% on average). It can be observed that the average measurement uncertainty seems to be smaller in the L cross-section than in the R and T cross-sections. The highest measurement uncertainty was calculated for linden and ash in the R section; they were 18%. The width of the confidence interval is related to the confidence level, the sample size, and the variability in the sample. We used a 95% confidence level and we performed twelve measurements for each tested combination: two measuring forces, three cross-sections, and six types of wood. The confidence intervals varied from 1% to 18%; this confirms the well-known high variability of wood properties [9].

Increasing hardness with increasing wood density was noticeable in all three cross-sections and at both measuring forces (Figure 6).

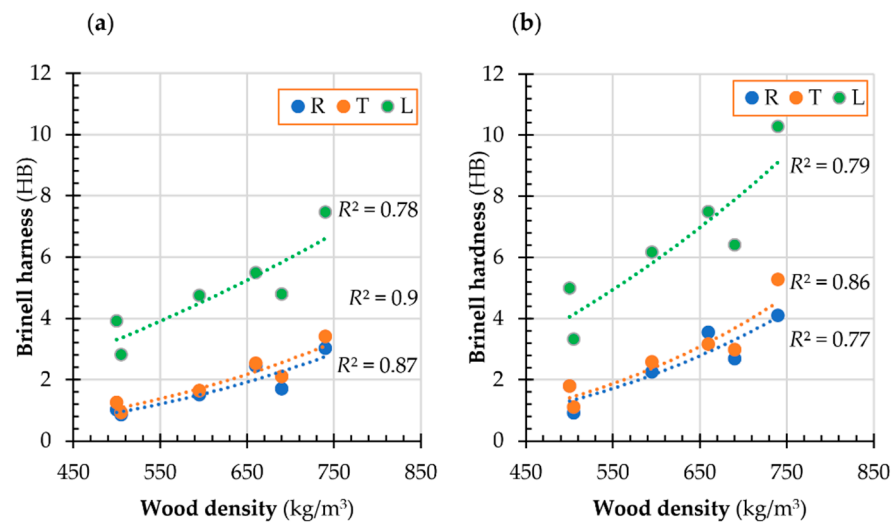


Figure 6. The Brinell hardness—wood density: (a)—30 kG measuring force, (b)—100 kG measuring force.

Figures 7–9 present the measured imprint depths. The tested wood species are arranged in ascending order according to their density, and the graphs show the two components of the total imprint depth. The permanent (plastic) imprint (h), which remains after the measuring force, is marked in blue, and the elastic component of the imprint’s depth (x) is marked in green, that is, the distance by which the imprint’s depth was decreased.

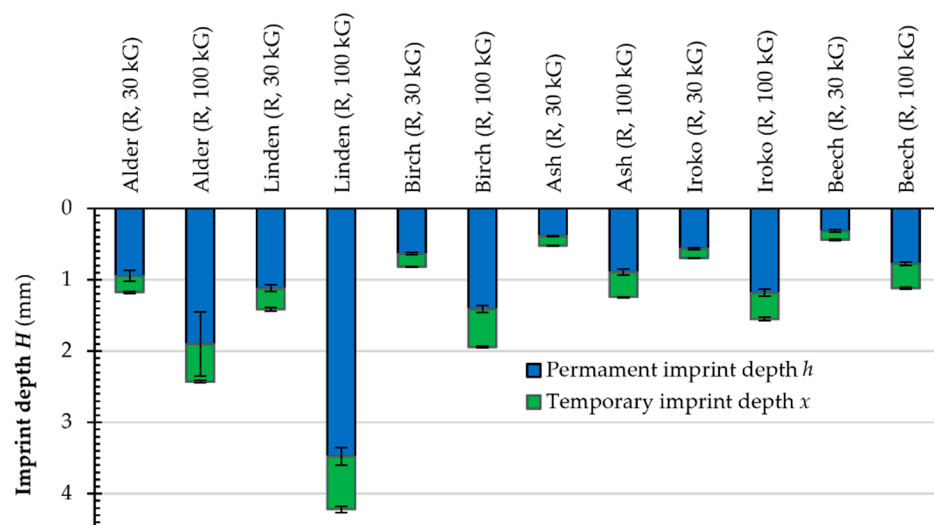


Figure 7. Imprint depth under measuring load (radial direction).

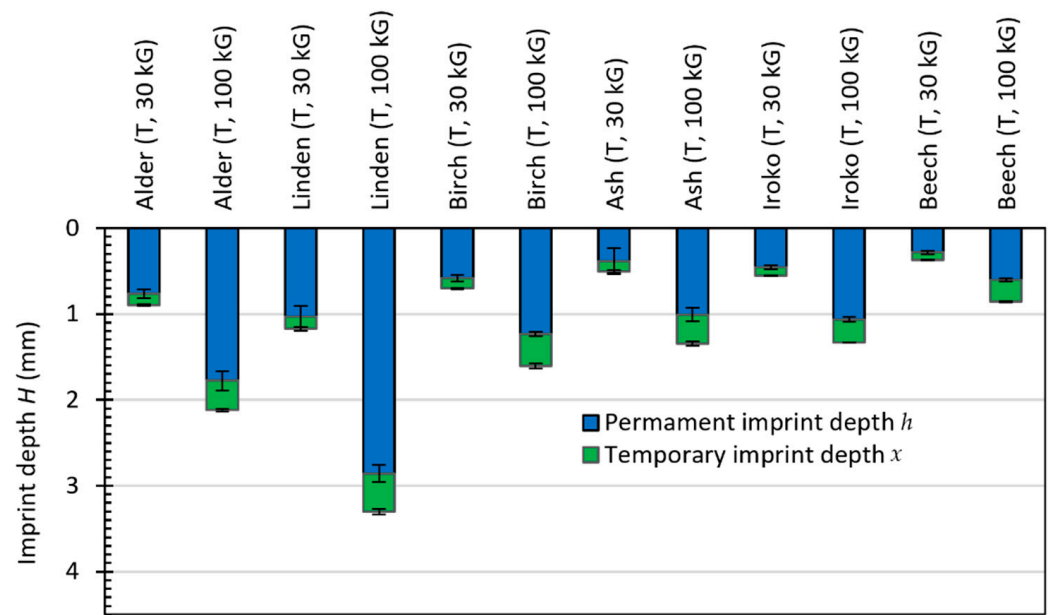


Figure 8. Imprint depth under measuring load (tangential direction).

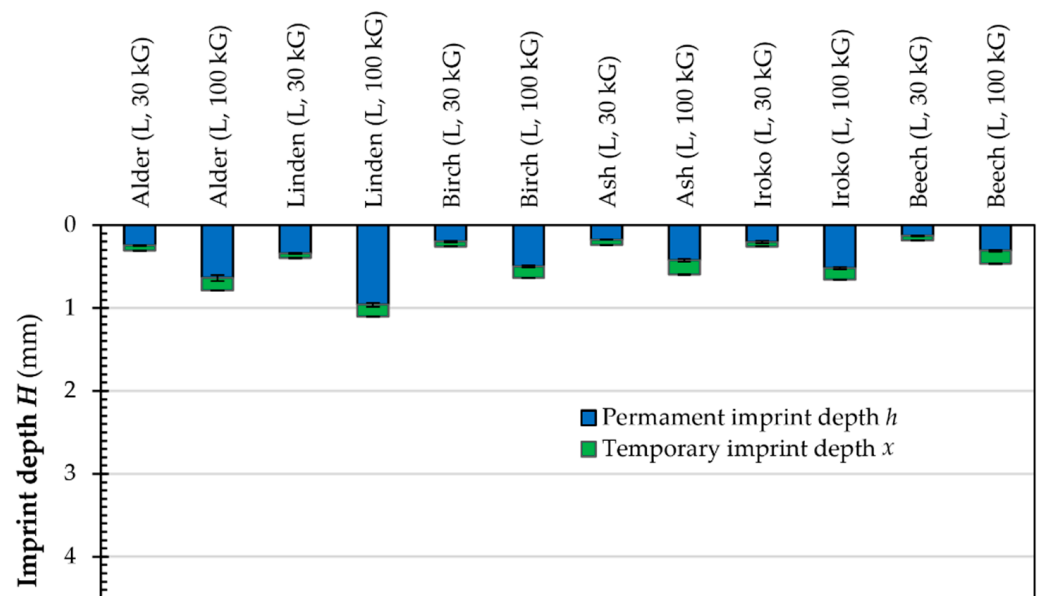


Figure 9. Imprint depth under measuring load (longitudinal direction).

Regarding the study’s primary aim, the most important is the permanent imprint depth (h) shares of the total imprint depth (H). These shares are shown in Figures 10–12 (the symbols R, T, L, and h , H are set out in Figures 1 and 4).

The imprint depths caused by the force of 30 kG (Figures 7–9) were from 2.1 to 3.0-times smaller than the imprint depth caused by the 100 kG measuring force. This proportion between the imprint depths was similar in all three main wood cross-sections (R, T, L). The depths of imprints in the R and T cross-sections were similar, while they were three-times greater than in the L cross-section.

The shares of permanent imprint depth h in the total imprint depth H (including the elastic component of deformation x) did not depend on the cross-section of wood (R, T, and L) and the measuring force value. In each studied case, they ranged from 70 to 80%.

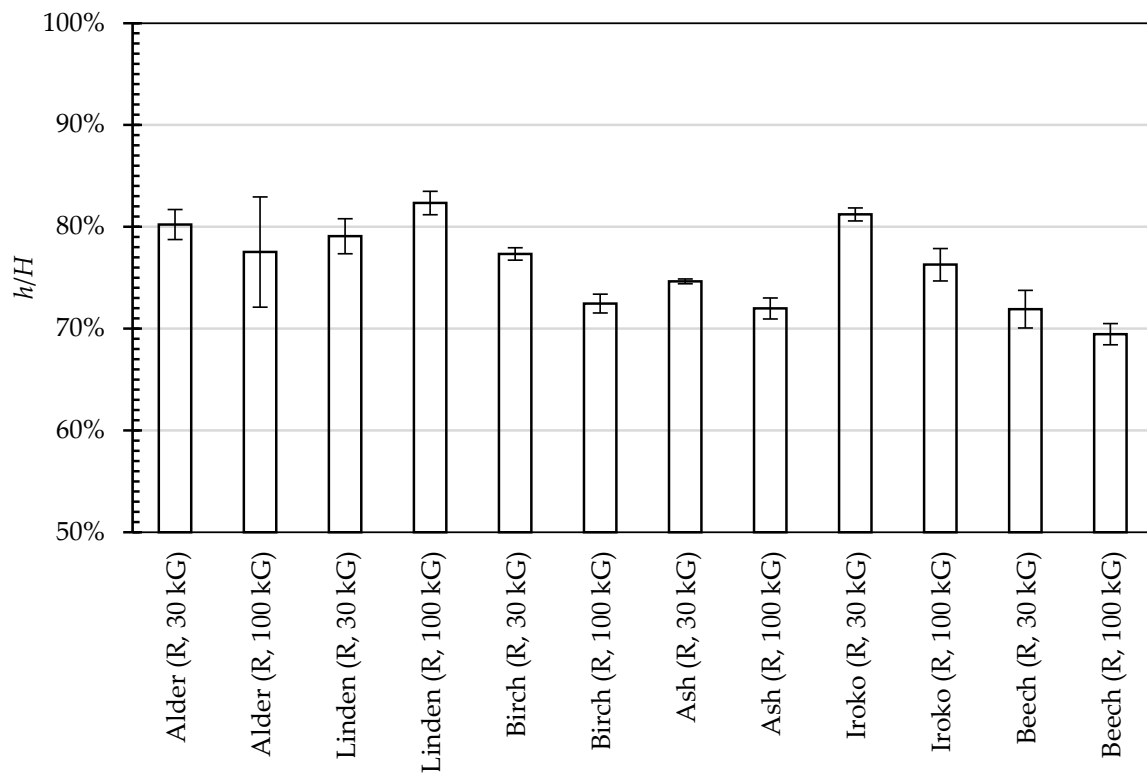


Figure 10. The R cross-section: the permanent imprint depth (h) shares the total imprint depth (H).

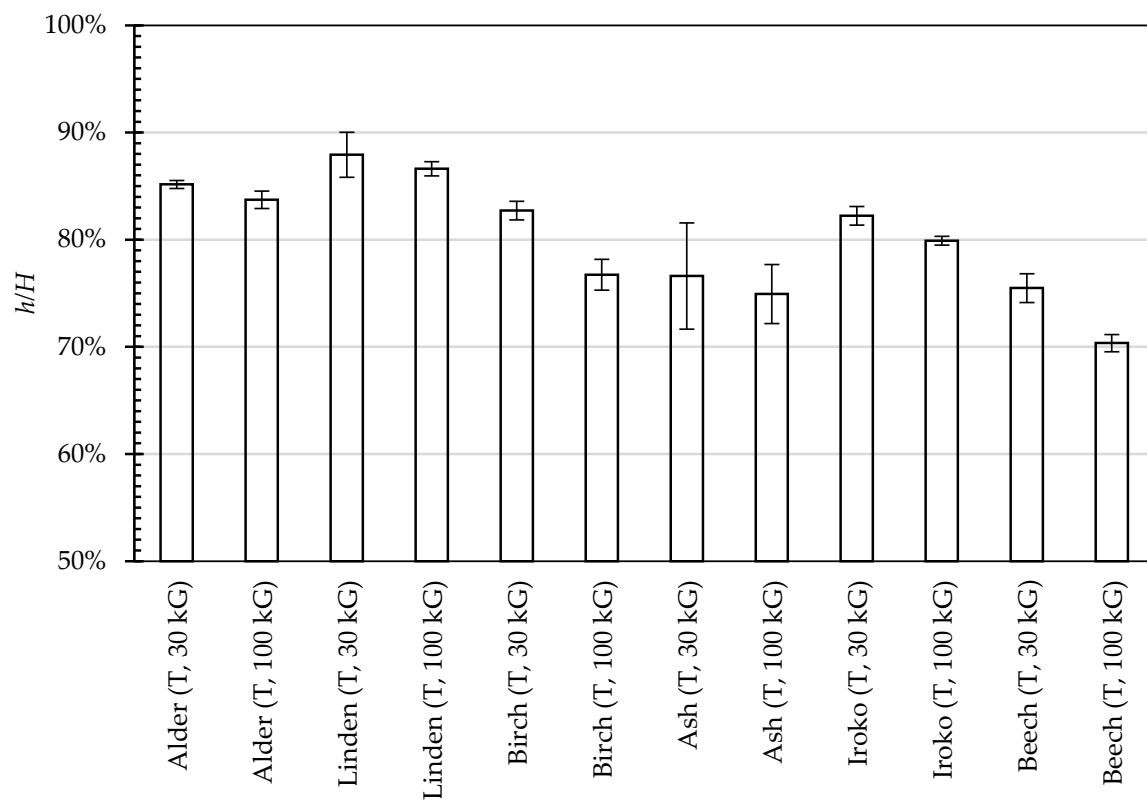


Figure 11. The T cross-section: the permanent imprint depth (h) shares the total imprint depth (H).

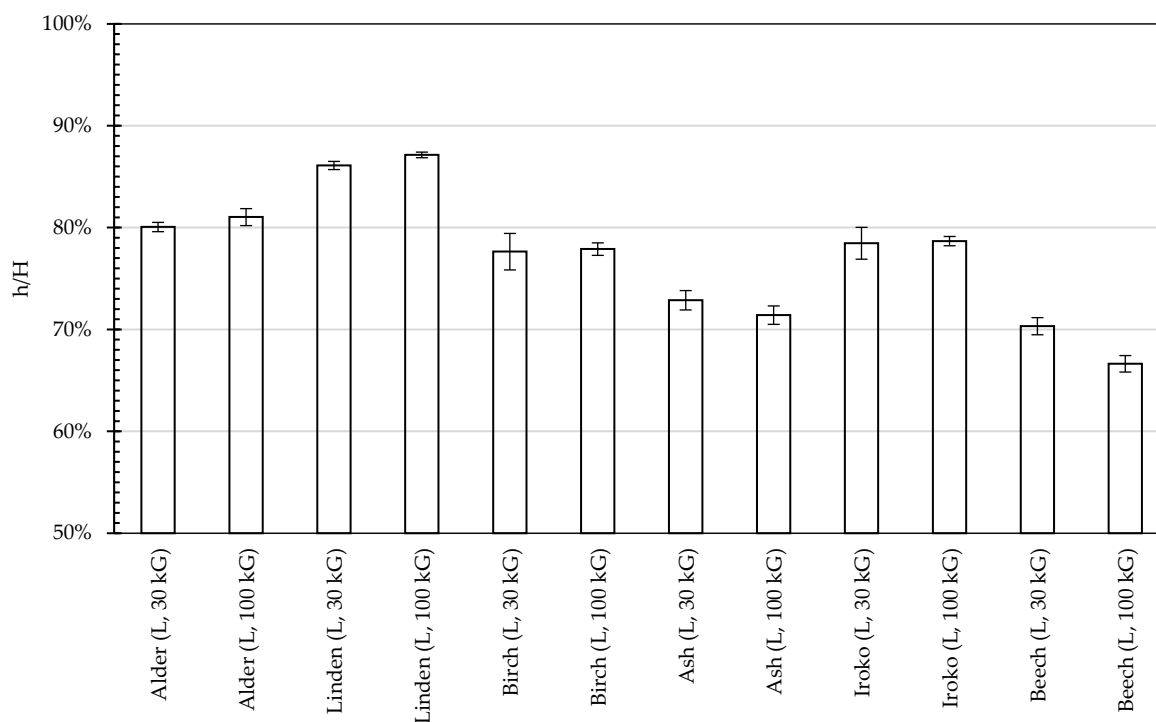


Figure 12. The L cross-section: the permanent imprint depth (h) shares of the total imprint depth (H).

4. Discussion

4.1. Hardness

The Brinell hardness of wood is associated with wood density [10], and it can be increased by increasing the density of the wood after pressing. Laskowska confirmed this possibility in tests involving the pressing of beech, oak, and pine wood, during which, after increasing the density of the samples by approximately 30%, the hardness increased by about 100% [13]. The hardness can also be reduced by reducing the strength of the wood after thermal modification [14]. Poplar wood, with a reduced modulus of elasticity (after thermo-modification at a temperature of 190–210 °C), had reduced hardness by about 25% [15]. Thermal modification influences the reduction of hardness in every main cross-section of wood differently: in the longitudinal cross-section by 3%, the radial cross-section by 15%, and the tangential cross-section by 25% [16]. The hardness is a property of the surface layer of the material [17], so the hardness of wood strongly depends on its density profile. Surface-densified pinewood shows an increased hardness and a high variation in measured hardness values, regardless of which testing method was used [18].

Our research confirms a well-known feature of wood mentioned in the Introduction: the hardness strongly depends on the cross-section of wood [9,10]. Our study obtained the highest hardness values in the longitudinal cross-section (L), perpendicular to the trunk axis (the end hardness of wood). The hardness was smaller in radial and tangential cross-sections (R and T—the side hardness of wood) (Figure 5). Those results are in line with the literature. For example, the radial hardness of Amboyna wood is 30–40% of the end hardness, and its tangential hardness is approximately 120–130% of the radial hardness (hardness R and T—a force of 20 kG was used; hardness L—a force of 50 kG was used) [19]. Our research confirms this regularity; hardness measured with 30 kG of all tested wood species was 26–45% and 104–124%, respectively, while hardness measured with 100 kG: 28–47% and 89–129%, respectively. In the case of beech wood, these values were 40 and 129% (force 100 kG). Similar hardness ratios were obtained in the experiment by Sedlar et al.: 42% and 126%, respectively (force 1000 N, 10 mm ball indenter) [16]. Table 2 shows the ratios of hardness measured in our tests in dependence of measuring force used and in dependence of directions to wood fibers.

Table 2. HB values ratios. Three main cross-sections of wood (R, T, and L) and two measuring forces.

Ratio	Equation	Wood Specie					
		Alder	Ash	Beech	Birch	Iroko	Linden
Hardness depending on the measuring force value	$HB_{(L, 100\text{ kG})} / HB_{(L, 30\text{ kG})}$	128%	136%	138%	134%	130%	118%
	$HB_{(R, 100\text{ kG})} / HB_{(R, 30\text{ kG})}$	157%	145%	136%	150%	159%	107%
	$HB_{(T, 100\text{ kG})} / HB_{(T, 30\text{ kG})}$	143%	125%	155%	157%	142%	119%
Hardness depending on the cross-section	$HB_{(R, 30\text{ kG})} / HB_{(L, 30\text{ kG})}$	26%	45%	41%	31%	36%	30%
	$HB_{(R, 100\text{ kG})} / HB_{(L, 100\text{ kG})}$	32%	47%	40%	35%	44%	28%
	$HB_{(R, 30\text{ kG})} / HB_{(T, 30\text{ kG})}$	123%	104%	113%	109%	124%	109%
	$HB_{(R, 100\text{ kG})} / HB_{(T, 100\text{ kG})}$	104%	89%	129%	114%	111%	122%

The measured HB values also depend on the measuring force used. We obtained the higher hardness values at a force of 100 kG. Similar observations were made by Koczan et al. [20], who described the results of wood hardness tests, among others, of beech wood. A potential explanation for the higher hardness values at 100 kG than at 30 kG is the strain hardening effect, which increases with a decreasing indentation of the measuring ball. This phenomenon was observed when measuring the hardness of metals [21]; in wood, the material’s cellular structure additionally influences it. Only after increasing the load did the plastic buckling of the cell walls reduce the volume of the voids and densify cell walls [22]. Based on the results of our research, the tested species can be classified into hard (ash, beech), medium-hard (alder, birch, iroko), and soft wood (linden) species. The influence of the measuring force value on the measured hardness was the lowest for soft species; it was (depending on the grain direction) from 118 to 107%. That influence ranged from 125 to 176% for the remaining wood species, as shown in Table 2. In the case of hardness measurements in the L cross-section, the influence of the force on hardness was the least diversified (118–138%); while in the R cross-section, this influence was the most diverse (107–176%).

4.2. Self-Re-Deformation

The ability to self-shallow the imprint after removing the measuring force (self-re-deformation) seems to depend on the density of the wood. A graphical representation of the self-re-deformation ability in the three main cross-sections of wood is presented in Figures 13–15.

The wood species with the highest density exhibited the highest ability of self-re-deformation. This is in line with our previous research [8] and reports from the literature [23]. In the case of the clear sapwood of kiln-dried Scots pine, the ability of side elastic self-re-deformation ranged from 45% (sphere-shaped indenter, 1000 N) for densified material to 91% (cylinder-shaped indenter, 2500 N) [24]. As shown in Figures 13–15, the ability to self-decrease in the depth of the imprint after removing the load in all main cross-sections (R, T and L) slightly increased with increasing wood densities. This tendency was observed for both measuring forces, 30 kG and 100 kG. In the R and T cross-sections, after the load is removed, the self-re-deformation ability was greater for the measuring force of 100 kG and less for the measuring force of 30 kG. In the L cross-section, the ability of self-re-deformation in the tested range depends only on the density of the wood (it does not depend on the value of the measuring force). These results show that the ability of self-re-deformation depends both on measuring force and the wood density in the R and T cross-sections; however, in the L cross-section, the ability of self-re-deformation depends on the wood density only. Overall, these results suggest the different progressions of cell-structure deformation in the R and T cross-sections compared to the L cross-section [25]. Cells are strongly elongated in the L direction; during compression in the R or T directions, they occur in the following sequence: (a) the linear-elastic bending of the cell walls, (b) the plastic buckling of the cell walls and reduction of void volume, and (d) cell walls are visco-elastically compressed (densification on a macroscopic level). The linear-elastic

bending of the cell walls is almost fully reversible, and the densification of cells is partially reversible. When the indenter is pressed in the R and T directions, the wood cells bend and collapse after reaching their plastic collapse load. Compression in the L direction (axially) causes the kinking of elongated cell walls in the L direction [26]. Kink (failed yield) occurs by local plastic buckling [27] or by the fracture of the cells' ends [28]. Local plastic buckling usually begins at points where the cells bend to make space for a ray [25]. Vural and Ravichandran described a similar deformation process of balsa wood cells under longitudinal compression. They related the course of deformation to wood density, stating that it is by the initial elastic and then plastic buckling of cell walls in low-density specimens, while kink band formation and end-cap collapse dominate in higher-density specimens [29]. This was also confirmed by the results of our research presented in Figures 13–15. Within the wood species, the tendency to self-re-deformation was generally higher for the measuring force of 100 kG (lower h/H). The only exception was found for the softest hardwood specie (linden), where a greater tendency to self-re-deformation was observed at the measuring force of 30 kG.

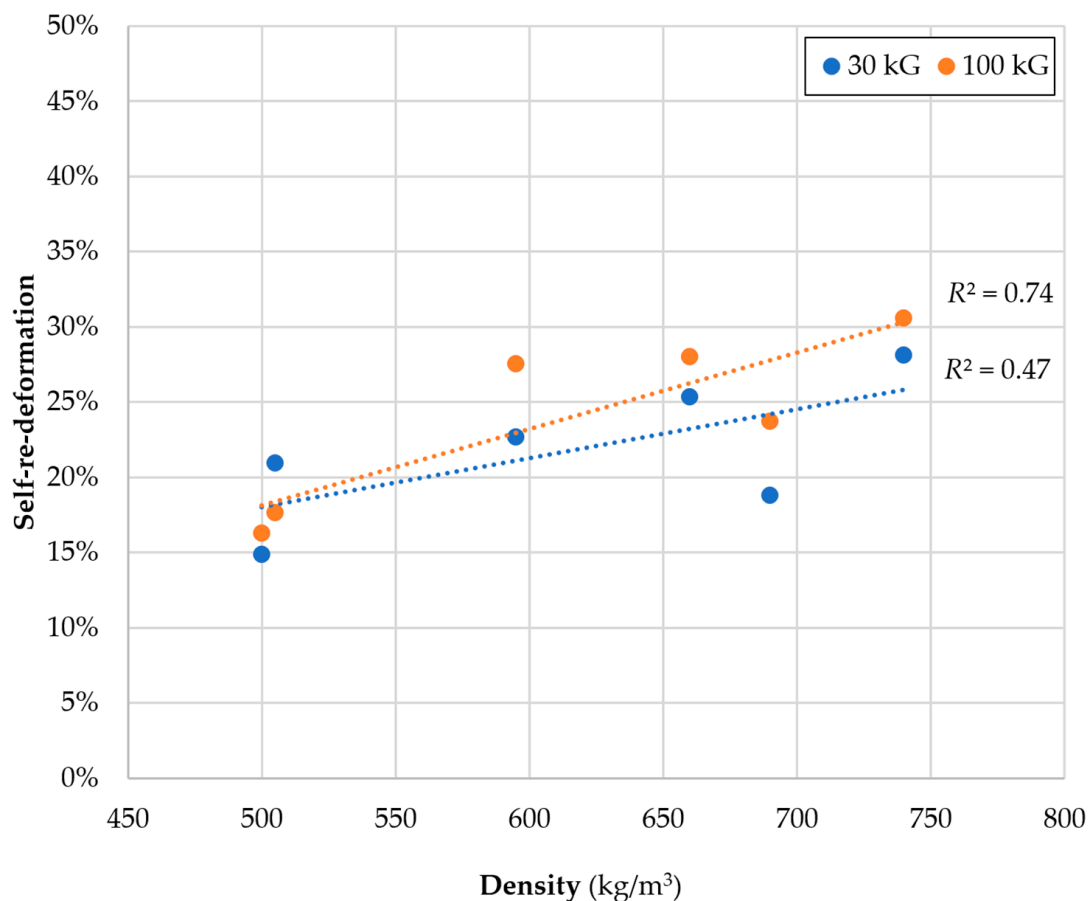


Figure 13. The ability of self-re-deformation in the R cross-section versus wood density.

The longitudinal strength of wood is always larger than the other two “directional” strengths, in part because the microfibrils of cellulose in the cell walls lie most nearly along the longitudinal direction, making the cells stiffer against longitudinal deformation [28,30]. In addition, a hexagonal prismatic wood cell is stiffer longitudinally (during compression) and less stiff transversely (in radial and tangential directions) because the thin cell walls bend [31]. The higher the density, the thicker the cell walls [9]. Therefore, density is an essential factor in predicting the strength of the wood.

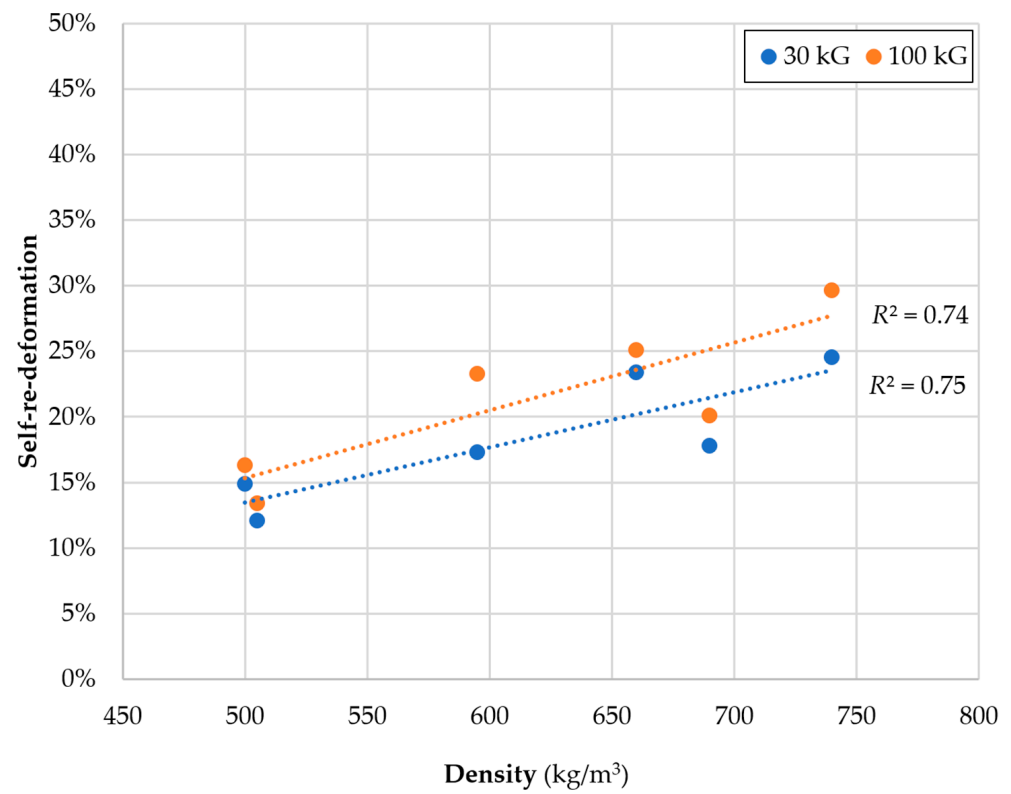


Figure 14. The ability of self-re-deformation in the T cross-section versus wood density.

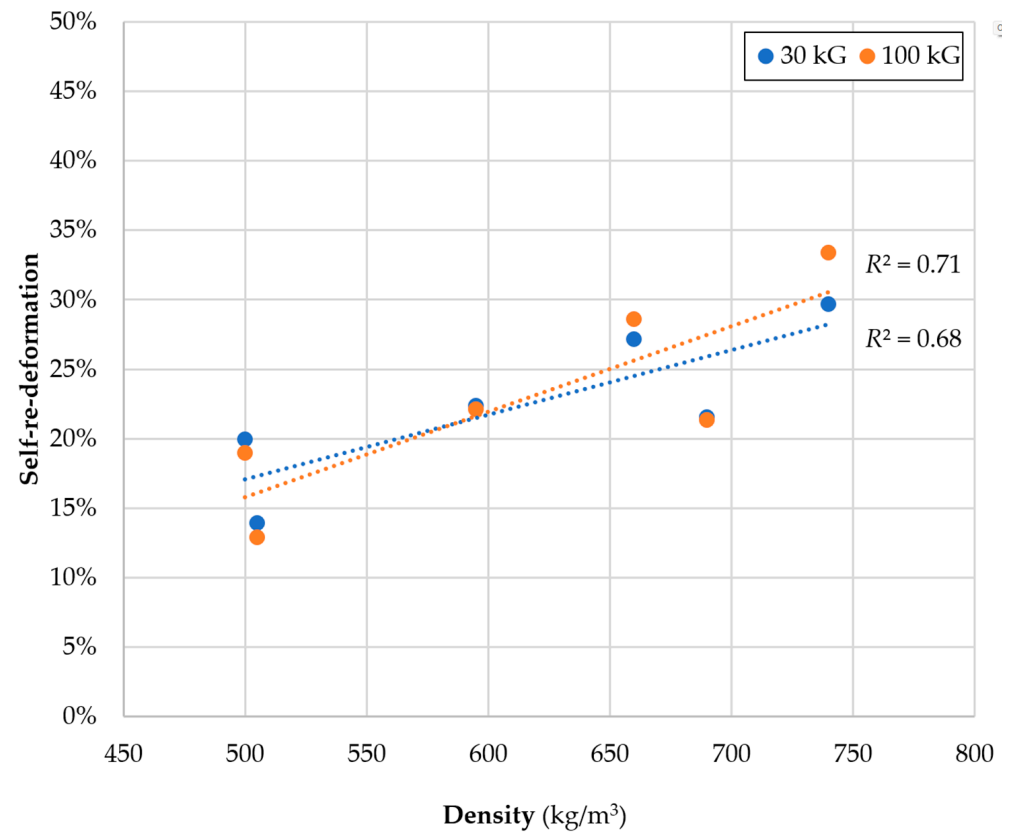


Figure 15. The ability of self-re-deformation in the L cross-section versus wood density.

5. Conclusions

- The greater the density of the wood, the highest Brinell hardness—and, at the same time, its tendency to self-re-deformation (self-shallowing of an imprint after the removal of the measuring force) is greater. The hardest tested wood species (beech) shows a share of the permanent imprint depth in the total imprint depth (h/H) only from 67 to 75%, while the wood with the lowest hardness (linden) from 82% to 88%. The self-re-deformation ability is thus linked to the wood density: the harder the wood, the smaller the share of the permanent imprint depth in the total imprint depth.
- The ability to self-re-deformation of all the tested wood species' radial and tangential cross-sections (R and T) depends on the wood density and the measuring force used. In contrast, in the longitudinal cross-section (L), this ability only depends on the wood density (the self-re-deformation ability is independent of the measuring force used). This observation shows that the compaction of the cell structure during side compression is largely reversible (semi-destructive), while the longitudinal deformation of the cell structure (the buckling of cell walls and fracture of ends of the cells) is irreversible (destructive).

Author Contributions: Conceptualization, M.S.; methodology, M.S. and G.P.; software, G.P.; validation, G.P. and M.S.; formal analysis, P.A., R.K., M.K. and T.R.; investigation, G.P.; resources, G.P. and M.S.; data curation, M.S.; writing—original draft preparation, M.S.; writing—review and editing, M.S., T.R. and P.A.; visualization, M.S. and G.P.; supervision, M.S.; project administration, P.A., R.K. and M.K.; funding acquisition, R.K. and M.K. All authors have read and agreed to the published version of the manuscript.

Funding: This research was supported by the Cultural and Educational Grant Agency of the Ministry of Education, Science, Research and Sport of the Slovak Republic under contract no. KEGA 026UMB-4/2021 and by the grant agency VEGA under project No. 1/0324/21 and project No. 1/0629/20. The study was also supported by the funding for statutory R&D activities as the research task No. 506.227.02.00 and No. 506.221.02.00 of the Faculty of Forestry and Wood Technology, Poznań University of Life Sciences.

Institutional Review Board Statement: Not applicable.

Informed Consent Statement: Not applicable.

Data Availability Statement: All data generated or analyzed during this study are included in this published article.

Conflicts of Interest: The authors declare no conflict of interest. The funders had no role in the study's design, in the collection, analyses, or interpretation of data, in the writing of the manuscript, or in the decision to publish the results.

References

1. Meyer, L.; Brischke, C.; Welzbacher, C.R. Dynamic and static hardness of wood: Method development and comparative studies. *Int. Wood Prod. J.* **2011**, *2*, 5–11. [[CrossRef](#)]
2. Liu, M.; Lin, J.; Lu, C.; Tieu, K.; Zhou, K.; Koseki, T. Progress in Indentation Study of Materials via Both Experimental and Numerical Methods. *Crystals* **2017**, *7*, 258. [[CrossRef](#)]
3. Broitman, E. Indentation Hardness Measurements at Macro-, Micro-, and Nanoscale: A Critical Overview. *Tribol. Lett.* **2017**, *65*, 23. [[CrossRef](#)]
4. Vörös, Á.; Németh, R. The History of Wood Hardness Tests. *IOP Conf. Ser. Earth Environ. Sci.* **2020**, *505*, 012020. [[CrossRef](#)]
5. *EN 1534: Wood Flooring and Parquet—Determination of Resistance to Indentation—Test Method*; European Committee for Standardization: Brussels, Belgium, 2020.
6. Niemz, P.; Stübi, T. Investigations of hardness measurements on wood based materials using a new universal measurement system. In *Symposium on Wood Machining, Properties of Wood and Wood Composites Related to Wood Machining*; Stanzl-Tschegg, S.E., Reiterer, A., Eds.; Christian-Doppler-Laboratory for Fundamentals of Wood Machining Institute of Meteorology and Physics, University of Agricultural Sciences: Vienna, Austria, 2000; pp. 51–61.
7. Lykidis, C.; Nikolakakos, M.; Sakellariou, E.; Birbilis, D. Assessment of a modification to the Brinell method for determining solid wood hardness. *Mater. Struct.* **2016**, *49*, 961–967. [[CrossRef](#)]

8. Sydor, M.; Pinkowski, G.; Jasińska, A. The Brinell Method for Determining Hardness of Wood Flooring Materials. *Forests* **2020**, *11*, 878. [[CrossRef](#)]
9. Kollmann, F.F.; Côté, W.A. *Principles of Wood Science and Technology. I Solid Wood*; Springer: Berlin/Heidelberg, Germany, 1968; ISBN 978-3-642-87930-2.
10. Möraht, E. Studien Über die Hygroskopischen Eigenschaften und die Härte der Hölzer. Habilitation Dissertation, Mitteilungen der Holzforschungsstelle an der Technischen Hochschule Darmstadt, Darmstadt, Germany, 1932.
11. Doyle, J.; Walker, J.C.F. Indentation hardness of wood. *Wood Fiber Sci.* **1985**, *17*, 369–376.
12. Hill, R.; Storåkers, B.; Zdunek, A. A theoretical study of the Brinell hardness test. *Proc. R. Soc. Lond. Math. Phys. Sci.* **1989**, *423*, 301–330.
13. Laskowska, A. Density profile and hardness of thermo-mechanically modified beech, oak and pine wood. *Drew. Prace Nauk. Doniesienia Komun.* **2020**, *63*, 26. [[CrossRef](#)]
14. Salca, E.-A.; Hiziroglu, S. Evaluation of hardness and surface quality of different wood species as function of heat treatment. *Mater. Des.* **2014**, *62*, 416–423. [[CrossRef](#)]
15. Zanuttini, R.; Negro, F.; Cremonini, C. Hardness and contact angle of thermo-treated poplar plywood for bio-building. *IForest Biogeosci. For.* **2021**, *14*, 274–277. [[CrossRef](#)]
16. Sedlar, T.; Šefc, B.; Stojnić, S.; Jarc, A.; Perić, I.; Sinković, T. Hardness of thermally modified beech wood and hornbeam wood. *Šumar. List* **2019**, *143*, 433. [[CrossRef](#)]
17. Sydor, M.; Wieloch, G. Construction Properties of Wood Taken into Consideration in Engenering Practice | Właściwości Konstrukcyjne Drewna Uwzględniane w Praktyce Inżynierskiej. *Drewno* **2009**, *52*, 63–73.
18. Scharf, A.; Neyses, B.; Sandberg, D. Hardness of surface-densified wood. Part 1: Material or product property? *Holzforschung* **2022**. [[CrossRef](#)]
19. Mijajima, H. Relation of the Hardness Number to the Applied Load in the Static Ball Indentation Test of Wood. *Nippon Rin Gakkai-Shi J. Jpn. For. Soc.* **1935**, *17*, 794–801. [[CrossRef](#)]
20. Koczan, G.; Karwat, Z.; Kozakiewicz, P. An attempt to unify the Brinell, Janka and Monnin hardness of wood on the basis of Meyer law. *J. Wood Sci.* **2021**, *67*, 7. [[CrossRef](#)]
21. Tabor, D. *The Hardness of Metals*; Oxford Classic Texts in the Physical Sciences; Clarendon Press, Oxford University Press: Oxford, UK; New York, NY, USA, 2000; ISBN 978-0-19-850776-5.
22. Gibson, L.J.; Ashby, M.F. *Cellular Solids: Structure and Properties*, 2nd ed.; Cambridge University Press: Cambridge, UK, 1997; ISBN 978-0-521-49911-8.
23. Heräjärvi, H. Variation of basic density and Brinell hardness within mature Finnish *Betula pendula* and *B. pubescens* stems. *Wood Fiber Sci.* **2004**, *36*, 216–227.
24. Rautkari, L.; Laine, K.; Kutnar, A.; Medved, S.; Hughes, M. Hardness and density profile of surface densified and thermally modified Scots pine in relation to degree of densification. *J. Mater. Sci.* **2013**, *48*, 2370–2375. [[CrossRef](#)]
25. Ashby, M.F.; Jones, D.R.H. *Engineering Materials 2: An Introduction to Microstructures, Processing and Design*, 3rd ed.; Butterworth-Heinemann: Oxford, UK, 2006; ISBN 978-0-08-046863-1.
26. Adusumalli, R.-B.; Raghavan, R.; Ghisleni, R.; Zimmermann, T.; Michler, J. Deformation and failure mechanism of secondary cell wall in Spruce late wood. *Appl. Phys. A* **2010**, *100*, 447–452. [[CrossRef](#)]
27. Zauner, M.; Stapanoni, M.; Niemz, P. Failure and failure mechanisms of wood during longitudinal compression monitored by synchrotron micro-computed tomography. *Holzforschung* **2016**, *70*, 179–185. [[CrossRef](#)]
28. Gibson, L.J. The hierarchical structure and mechanics of plant materials. *J. R. Soc. Interface* **2012**, *9*, 2749–2766. [[CrossRef](#)] [[PubMed](#)]
29. Vural, M.; Ravichandran, G. Microstructural aspects and modeling of failure in naturally occurring porous composites. *Mech. Mater.* **2003**, *35*, 523–536. [[CrossRef](#)]
30. Thibaut, B.; Gril, J.; Fournier, M. Mechanics of wood and trees: Some new highlights for an old story. *Comptes Rendus Acad. Sci. Ser. IIB Mech.* **2001**, *329*, 701–716. [[CrossRef](#)]
31. Easterling, K.; Harrysson, R.; Gibson, L.; Ashby, M.F. On the mechanics of balsa and other woods. *Proc. R. Soc. Lond. Math. Phys. Sci.* **1982**, *383*, 31–41. [[CrossRef](#)]